



1 Recovery of stratigraphic data with associated uncertainties from drillhole databases using litho2strat  
2 1.0

3 Vitaliy Ogarko<sup>1,2</sup> and Mark Jessell<sup>1,2</sup>

4 <sup>1</sup>Centre for Exploration Targeting (School of Earth Sciences), The University of Western Australia,  
5 Crawley, 6009 WA, Australia

6 <sup>2</sup>Mineral Exploration Cooperative Research Centre, The University of Western Australia, Crawley,  
7 6009 WA, Australia

8 Correspondence: Vitaliy Ogarko ([vitaliy.ogarko@uwa.edu.au](mailto:vitaliy.ogarko@uwa.edu.au))

9

10



## Abstract

11

12

13 Australian commonwealth, state and territory geological surveys possess information on over 3  
14 million drillhole logs. There are many more wells drilled in the search for oil and shallower holes  
15 related to hydrogeology. Other countries no doubt have similar data holdings. Together these legacy  
16 drillhole datasets have the potential to significantly improve our subsurface data coverage but have  
17 limited use as constraints on regional 3D geological models as many if not most drill logs lack  
18 stratigraphic information.

19 This study develops open-source codes and methodologies for stratigraphy recovery from drillhole  
20 databases by introducing a correlation algorithm that integrates data from multiple drillholes. The  
21 algorithms combine constraints from lithological descriptions, with stratigraphic relationships  
22 automatically derived from regional maps. In addition, by integrating uncertainty quantification and  
23 presenting multiple geological hypotheses, the resulting stratigraphical description provide critical  
24 insights for resource estimation, scenario analysis, and data acquisition strategies.

25 The application of our method to a dataset of 52 drillholes from South Australia demonstrated its  
26 ability to make useful predictions of stratigraphic solutions and quantifying associated uncertainties.  
27 These results not only validate our approach but also highlight opportunities to refine current  
28 stratigraphic descriptions and provide a valuable new source for regional 3D geological modelling.

29

30



## 31 1. Introduction

32

33 Drillhole data serves as a fundamental constraint for subsurface geological exploration and 3D  
34 geological modelling, offering direct insights into lithological and hence stratigraphic features  
35 (Wellmann & Caumon, 2018). However, the inherent sparsity of such data, coupled with challenges  
36 posed by legacy datasets maintained by industry and Geological Survey Organizations (GSOs), often  
37 hinders comprehensive geological understanding and modelling (Jessell et al., 2010; Pakyuz-Charrier  
38 et al., 2018). GSOs' databases typically contain complexly coded lithological information but limited  
39 stratigraphic data, creating a critical gap in the data needed for accurate and meaningful geological  
40 predictions (Hartmann & Moosdorf, 2012).

41 Geological modelling plays a crucial role in understanding subsurface structures and processes,  
42 providing a foundation for various applications in earth sciences (M. Jessell et al., 2014). Such  
43 modelling commonly relies on datasets such as borehole data, geophysical data, and mapping data.  
44 From these, borehole data provide the most accurate insights into subsurface geology and stratigraphy  
45 (Guo et al., 2022). The models generated through geological modelling can serve dual purposes: they  
46 can be directly employed for geological interpretations, such as identifying fault systems, and mineral  
47 deposits (Alvarado-Neves et al., 2024; Vollgger et al., 2015), or they can be integrated as constraints in  
48 methodologies that use a prior 3D model, such as geophysical inversions (Giraud et al., 2017; Martin  
49 et al., 2024; Ogarko et al., 2021; Tarantola, 2005) and hydrogeological forward modelling (D'Affonseca  
50 et al., 2020). By incorporating geological models into geophysical inversion, it is possible to refine the  
51 interpretation of subsurface properties and achieve greater accuracy in representing complex  
52 geological environments.

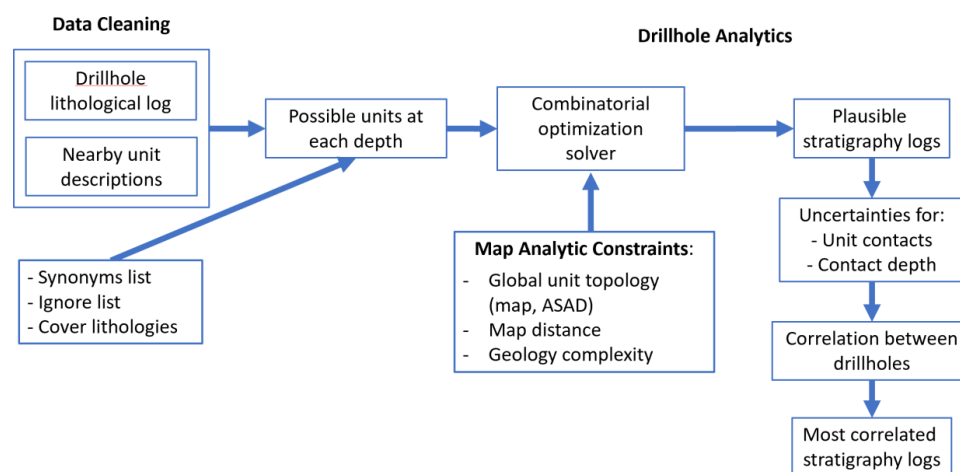
53 Modern drillhole measurement techniques primarily focus on chemical, mineralogical and lithological  
54 characterization, whereas the fundamental categorical unit of regional 3D geological models is defined  
55 by its stratigraphy (Calcagno et al., 2008; Caumon et al., 2009; Mallet, 2002). This discrepancy  
56 underscores the need for innovative approaches to recover and integrate stratigraphic information  
57 from existing datasets. Recent advancements in automation, particularly through machine learning  
58 and natural language processing, have demonstrated significant potential in addressing these  
59 challenges by standardizing and extracting lithological and stratigraphic data at scale (Guo et al., 2024;  
60 Joshi et al., 2021; Schetselaar & Lemieux, 2012).

61 This study develops open-source codes and methodologies for stratigraphy recovery from drillhole  
62 databases by introducing a correlation algorithm that integrates data from multiple drillholes, we  
63 enhanced the robustness and reliability of stratigraphic interpretations. By integrating uncertainty  
64 quantification and presenting multiple geological hypotheses, the resulting stratigraphical description  
65 provide critical insights for resource estimation, scenario analysis, and data acquisition strategies. The  
66 application of our method to a dataset of 52 drillholes from South Australia demonstrated its ability to  
67 make useful predictions of stratigraphic solutions and quantifying associated uncertainties. These  
68 results not only validate our approach but also highlight opportunities to refine current stratigraphic  
69 descriptions, improving workflow accessibility and paving the way for more effective geological  
70 assessments and decision-making processes.



## 71 2. Methodology

### 72 2.1 Workflow



73

74 Figure 1: The different stages of the analysis.

75 The workflow shown in Fig. 1 consists of 5 key steps grouped into three main tasks: Data Cleaning  
 76 (using the dh2loop code), Map Analytic Constraints (using map2loop and custom codes developed  
 77 for this project) and Drillhole Analytics (using the litho2strat code developed for this project).

78

#### 79 2.1.1 Data Cleaning

80 Prior to analysing the drillhole data we went through a number of automated data cleaning and  
 81 harmonisation steps.

82 a) Harmonisation of drillhole lithology descriptions using the dh2loop code described in (Joshi et  
 83 al., 2021) (code available here: <https://github.com/Loop3D/dh2loop>) This enables us to  
 84 produce a standardised lithological description for multiple drillholes in a region, regardless of  
 85 their provenance. This includes the use of a synonym list ("granite" vs "granitoid"), and ignore  
 86 list (e.g. "fault") together with a list of cover lithology terms (e.g. "saprolite") that enables us  
 87 to simplify the list of terms and exclude irrelevant information.

88

89 b) Harmonisation of lithological descriptions for formations described in the geological map of  
 90 the target area. This ensures that the same terminology is used for borehole lithological  
 91 descriptions and map lithologies.

92 Together steps a & b provide a list of possible units at each depth down a drill hole.

93

#### 94 2.1.2 Map Analytic Constraints

95 a) Calculation of the distance between each polygon in a map and the target borehole. A custom  
 96 Python script was developed. This information can be used as a guide to the likelihood that a  
 97 drillhole would intersect a given unit.

98



99        b) We then used the map2loop engine (M. Jessell et al., 2021) (code available here:  
100        <https://github.com/Loop3D/map2loop> ) to extract the topological relationships between the  
101        surface expression of stratigraphic different units. This would later be used to assess the  
102        likelihood that two units would be in contact in the drillhole.

103  
104        Unit connectivity information can also be obtained from the Australian Stratigraphic Units  
105        Database (ASUD) as well as from various published reports containing stratigraphic data. The  
106        ASUD serves as a comprehensive repository of geological information, providing valuable  
107        insights into the relationships between different stratigraphic units across Australia.  
108        Additionally, numerous geological surveys and research studies offer stratigraphic data that  
109        can further enrich our understanding of unit connectivity. By leveraging this information, we  
110        can enhance our stratigraphic models, improve the accuracy of correlations between  
111        drillholes, and facilitate a deeper understanding of the geological framework in specific  
112        regions.

113

114        These two steps allow us to capture information on the spatial and topological relationships  
115        between the mapped units.

116

### 117    **2.1.3 Drillhole Analytics**

118        a) In this stage of the analysis, we developed a new code called litho2strat (code available here:  
119        <https://github.com/Loop3D/litho2strat>; Ogarko et al., 2025). The information about code  
120        design is detailed in Section 2.4. The code uses a combinatorial optimisation solver as  
121        follows:

122        - We employed a Branch and Bound algorithm, which is a powerful method for solving  
123        optimization problems (Land & Doig, 1960). This approach systematically enumerates all  
124        potential candidate solutions by exploring the state space.

125        - New branches could be added while traversing the drillhole log from top to bottom, using a  
126        list of possible units at each depth down a drill hole and a unit topological relationship.

127        - We applied bounds by adding solution constraints. The branch is discarded if it does not  
128        satisfy the constraints. The types of constraints we apply are discussed in Section 2.2.

129        - In the end, we could obtain a plausible set of solutions fitting the data and satisfying the  
130        constraints. This strategy not only ensures a thorough exploration of the solution space but  
131        also optimizes efficiency by eliminating unnecessary computations, ultimately leading to a  
132        more effective and streamlined search process.

133        - Finally, we calculated the uncertainties directly from the whole set of solutions.

134        b) In this stage, we employ the litho2strat code to establish correlations between drillholes,  
135        which helps to reduce uncertainty in the calculated set of plausible stratigraphic solutions.  
136        The correlated solution scores are assigned based on overall uncertainty, with solutions  
137        receiving the highest scores selected as the most plausible options. For further details on the  
138        correlation algorithm utilized, please refer to Section 2.3.

139



## 140 2.2 Solution constraints

141

142 For the Branch and Bound (BnB) algorithm, providing efficient constraints (bounds) is crucial for  
143 generating geologically plausible stratigraphies and reducing the search space. Without these  
144 bounds, the BnB algorithm reverts to exhaustive search, which is less efficient. We utilize two types  
145 of solution constraints: the first can be derived from geological maps (as discussed in the ‘Map  
146 Analytic Constraints’ section), while the second is selected by the user based on the expected  
147 geological complexity of the area (e.g., the presence of known faults).

148 The specific constraints employed include:

- 149 1. **Distance from the Drillhole to the Unit:** This constraint limits the number of geological units  
150 considered in the calculations, ensuring relevance to the drillhole’s location.
- 151 2. **Global Unit Connectivity:** This constraint restricts the potential contacts between units,  
152 enhancing the accuracy of the stratigraphic model.
- 153 3. **Top Unit Constraint:** Information regarding the top unit can be extracted from geological  
154 maps, providing a foundational boundary for the stratigraphy.
- 155 4. **Solution Complexity (Occurrence):** This constraint sets a maximum limit on how many times  
156 a unit can appear in the final stratigraphy. For example, in the presence of a fault, the same  
157 geological unit may appear twice within the same log.
- 158 5. **Solution Complexity (Contacts):** This constraint defines the maximum number of unit  
159 contacts allowed within a continuous sequence of drillhole lithologies. For instance, in a  
160 continuous sequence of “sandstone” lithologies, different sandstones may belong to  
161 separate geological units.

162 These constraints work together to enhance the efficiency and effectiveness of the BnB  
163 algorithm, ensuring that the resulting stratigraphies are both plausible and reflective of the  
164 geological context.

165

## 166 2.3 Solution correlation

167

168 We utilize solution correlation analysis to establish relationships between multiple drillholes, serving  
169 as a constraint on the plausibility of stratigraphic ordering. This correlation can be applied either to  
170 stratigraphy logs or to the topological relationships of units, represented through connectivity  
171 graphs.

172 A key challenge in correlating stratigraphy logs is that units at the same depth may not align across  
173 different drillholes, mainly due to variations in unit dip and thickness. To address this, we focus on  
174 correlation based on topological relationships. Connectivity graphs are constructed for each drillhole  
175 using a plausible set of stratigraphic solutions derived from the Branch and Bound (BnB) solver.

176 In these graphs, the edges are weighted by the probability of unit contacts, calculated as the number  
177 of solutions that include a specific unit contact divided by the total number of solutions for that  
178 drillhole. This approach enhances the accuracy of the correlations, providing a more reliable  
179 framework for establishing stratigraphic relationships.



180 We propose the correlation algorithm as follows:

- 181 I. **Calculate Solution Scores:** For each solution  $i$ , compute the solution score  $S(i, G_{self})$  using  
182 the connectivity graph from the current drillhole  $G_{self}$ . This score is defined as the sum of  
183 the edge weights for all solution contacts, indicating the likelihood of the solution within the  
184 current drillhole.
- 185 II. **Calculate External Solution Scores:** For each external drillhole  $j$ , calculate the solution scores  
186  $S(i, G_{ext}^j)$  using their respective connectivity graphs. This score reflects the likelihood of the  
187 solution for each external drillhole.
- 188 III. **Build Final Correlated Solution Score:** Construct the final correlated solution score  $C(i)$   
189 using the following formula:

$$190 \quad C(i) = \frac{S(i, G_{self}) + \sum_{j=1}^{N-1} S(i, G_{ext}^j)}{N}$$

191 This final score represents the overall likelihood of the solution across all drillholes,  
192 effectively correlating the current solution with all solutions from the external drillholes  
193 based on the topological relationships of the geological units.

194 The final correlated solution score provides a means to assign correlated scores to various solutions,  
195 effectively altering their ranking within the overall assessment. This adjustment not only enhances  
196 the clarity of which solutions are more viable but also helps to reduce uncertainty associated with  
197 those solutions. By refining the evaluation process in this manner, we can achieve a more precise  
198 understanding of the relationships between different geological units. By integrating and correlating  
199 drillhole data effectively, we ensure that the stratigraphic framework accurately reflects the natural  
200 variations and interconnections present in the subsurface. This consistency is essential for making  
201 informed decisions in geological exploration ultimately leading to more reliable outcomes in our  
202 geological interpretations.

203 In the proposed correlation algorithm, we can select between summation and multiplication for  
204 calculating the correlated score in step iii. Summation is less sensitive to outliers; for instance, if one  
205 drillhole in the set has a zero score, using multiplication would result in a total score of zero.  
206 Additionally, we can apply weighting to different drillholes, such as by using geological distance, to  
207 reduce the influence of more distant drillholes on the overall score.

208 Moreover, it's important to note that the algorithm exhibits linear scalability with respect to the  
209 number of drillholes. This efficiency is achieved by utilizing solution connectivity graphs rather than  
210 evaluating each pair of solutions individually, which can be computationally expensive.

211

## 212 2.4 Code design

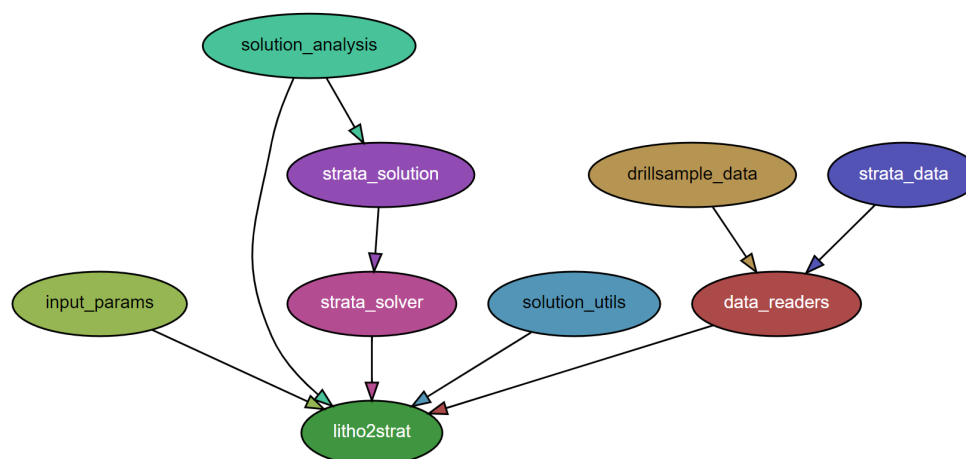
213

214 A Python package called litho2strat has been developed for stratigraphy recovery. It can be easily  
215 installed using the command "pip install", and it has minimal external library dependencies: numpy,  
216 matplotlib, and NetworkX. The NetworkX library is utilized to create a directed graph data structure  
217 that represents the topological relationships of relative unit ages (Hagberg et al., 2008). It also  
218 supports exporting graphs to GML format (Himsolt, 1997) for advanced graph visualization with tools  
219 like yEd (<https://www.yworks.com/products/yed>).



220 Interaction with the code is facilitated through a *Parfile*, a text file that contains all necessary  
221 parameters and paths to the input data files. The parameters in the *Parfile* are organized into several  
222 categories based on their functionality, including input file paths, solver settings, and data  
223 preprocessing options. An example of such a *Parfile* is provided in Appendix A.

224 The code architecture efficiently organizes distinct modules, including data reader, the user interface  
225 (represented by the *Parfile*), the algorithms (such as the solver), and the visualization components  
226 (e.g., output figures and graphs), as shown in Fig. 2. This design enhances code readability, making it  
227 easier for developers to understand and navigate the codebase. Additionally, it facilitates further  
228 extensions by allowing new features to be integrated seamlessly. The structure also supports  
229 effective testing, ensuring that modifications can be verified without introducing errors.



230

231 Figure 2: The module dependencies of the *litho2strat* code. The graph is generated by the *pydeps*  
232 utility, while excluding external dependencies.

### 233 3. Example Use

234

235 For this example, we used a set of 52 drillholes from South Australia originally drilled by Teck  
236 Cominco Pty. Ltd. (Fig. 3). This area was chosen as there were a number of holes equally spaced with  
237 a relatively homogenous spatial distribution and the holes provided both lithological logs and  
238 existing interpretations of the down-hole stratigraphy.



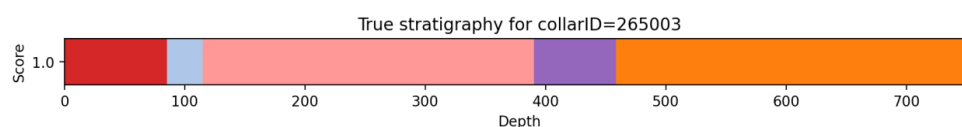
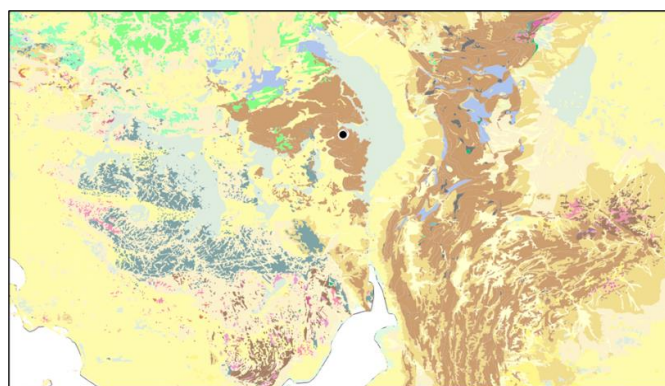


Figure 3: Location of South Australia test area, together with an example stratigraphic log.

## Data Cleaning

Examples of terms in the ignore list for this case study include:

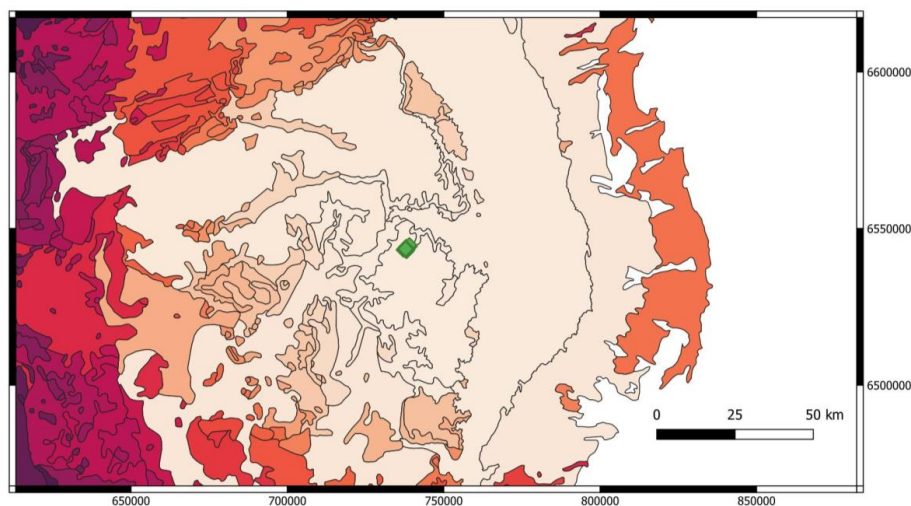
Breccia · (Undiff. · Origin)¶  
 Ironstone · (Metasomatic)¶  
 No · Information¶  
 Solution-Collapse · Breccia¶  
 Vein · (Undifferentiated)¶

Examples of the thesaurus of synonyms for this case study area include:

dolomite, · dolomite · rock, · carbonate · rock, · limestone¶  
 conglomerate, · diamictite¶  
 grit, · sandstone, · quartzite, · siltstone¶  
 gabbro, · gabbronorite¶

## Map Analytics

The figure below shows stratigraphic units coloured as a function of the distance to one of the drillholes (Fig. 4). A large search area was used for this example as the stratigraphy is fairly flat lying so there is no guarantee that a unit will reach the surface in the local neighbourhood.



252

253 Figure 4. Distant of stratigraphic units to drillholes (darker signifies larger distance). Green diamonds  
254 show the location of the drillholes.

255 In the initial analysis we plotted a network graph of all know topological relationships between  
256 stratigraphic units based on the geology map (extending out 100 km from the test area), the ASUD  
257 database, and additional information from published reports (Fig. 5).

258

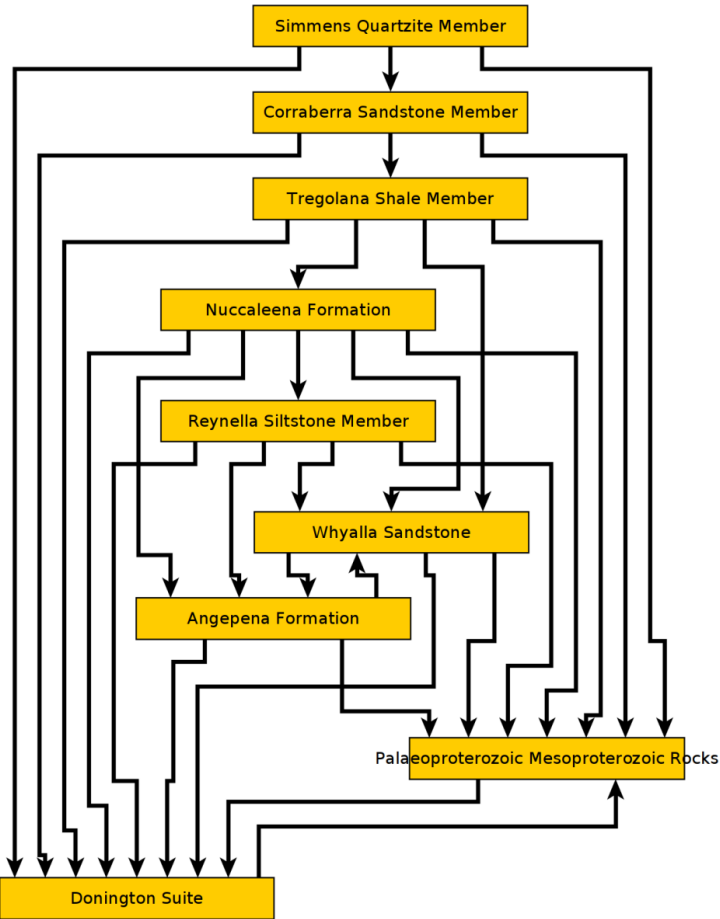


Figure 5: Topological relationships between units in and around the test area.

### Drillhole Analytics

The drillholes analysis calculated every possible stratigraphic ordering that was consistent with the observed lithological ordering down the drillhole and solution constraints (described in Sec. 2.3). By collating the results for all possible solution paths, we can produce estimates of the probability that any depth interval will be a particular stratigraphic unit (Fig. 6).

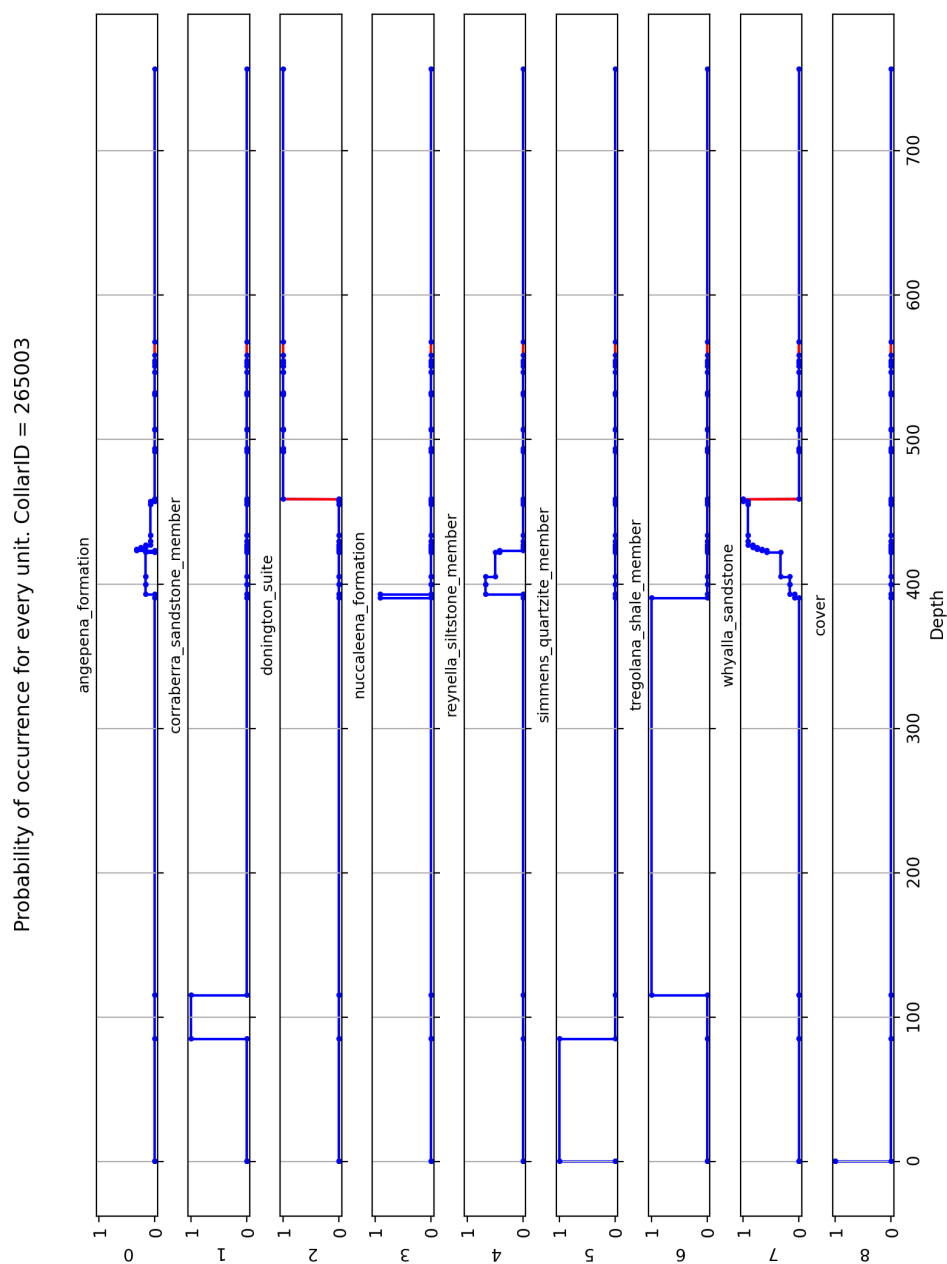
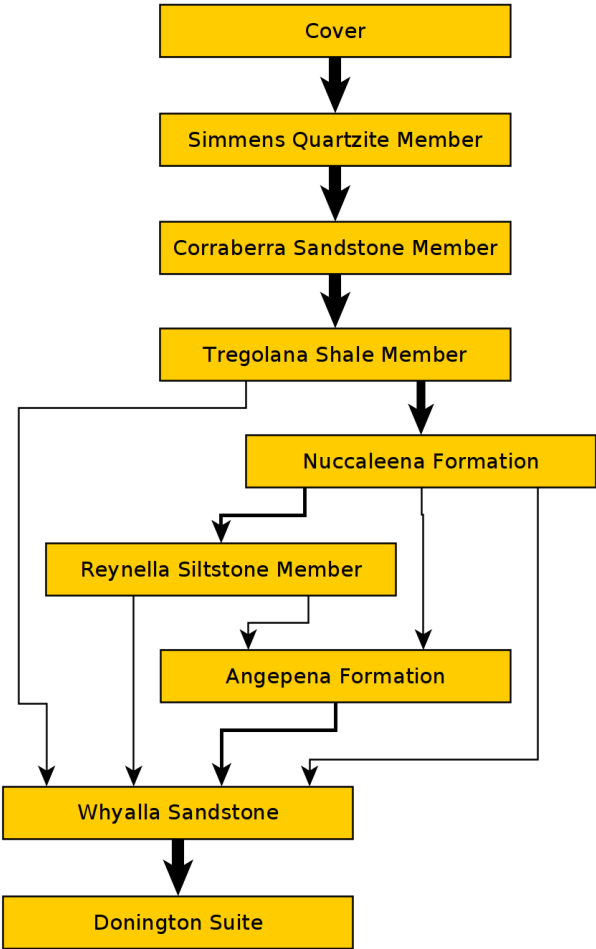


Figure 6: Estimated probability of each stratigraphic unit occurring at a given depth for a single drillhole.

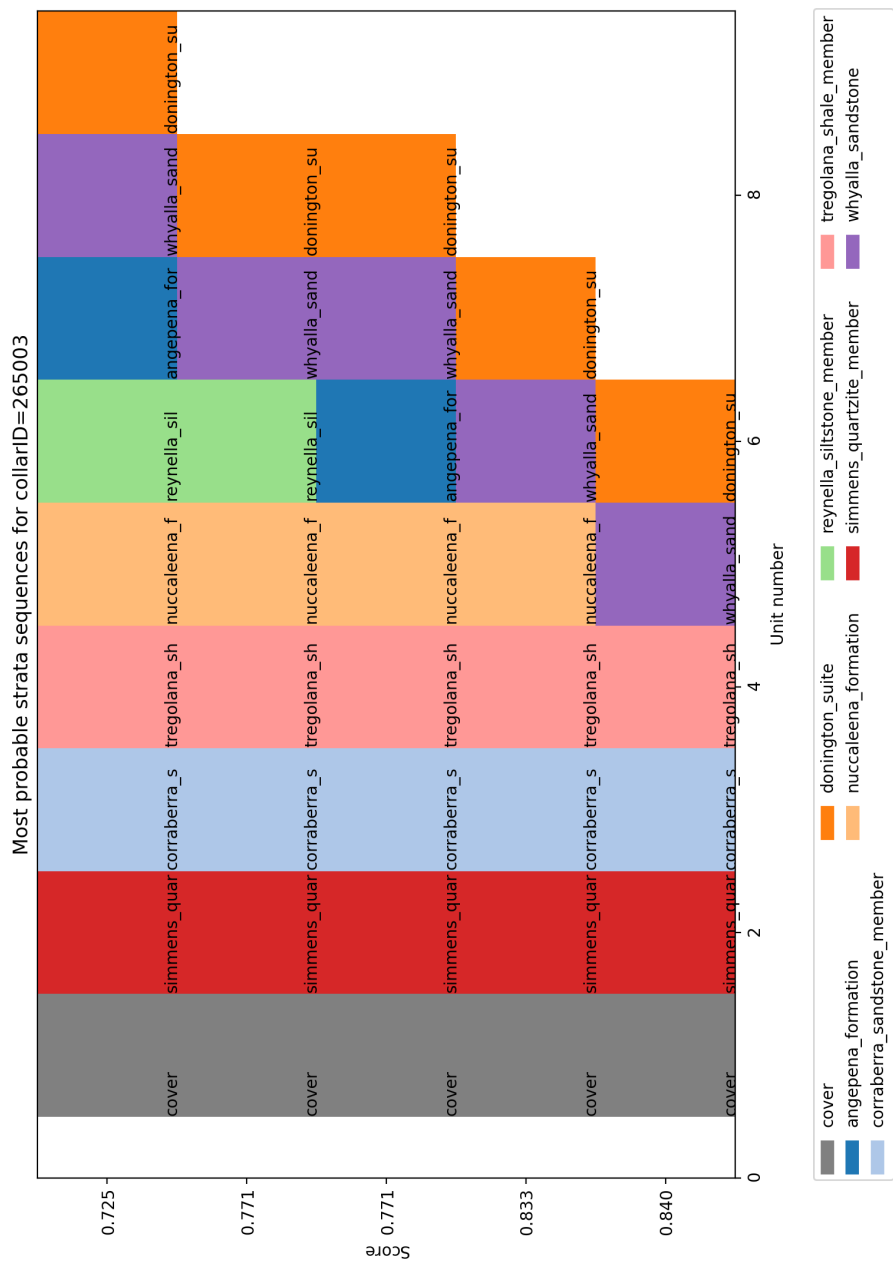
In Fig. 7, we present the final (local) unit connectivity derived from the stratigraphy solutions generated. The width of the graph edges indicates the probability of unit contacts, with thicker edges



273 signifying higher probabilities. This visual representation allows for a clear comparison of  
274 connectivity before (Fig. 6) and after the stratigraphic analysis.



275  
276 Figure 7: Calculated local topology using all solutions. Graph edges (relationships) between two  
277 stratigraphic units are displayed as a probability of a that contact-relationship occurring.  
278 The final solution score for a single ordering is calculated by summing of the probabilities of the  
279 contact edge weights. This allows us to sort the orderings by probability, ignoring stratigraphic  
280 thickness for now (Fig. 8).



281

282 Figure 8: The 5 most probable stratigraphic orderings, with their solution probability on the x axis  
283 and order of depth on the y axis.

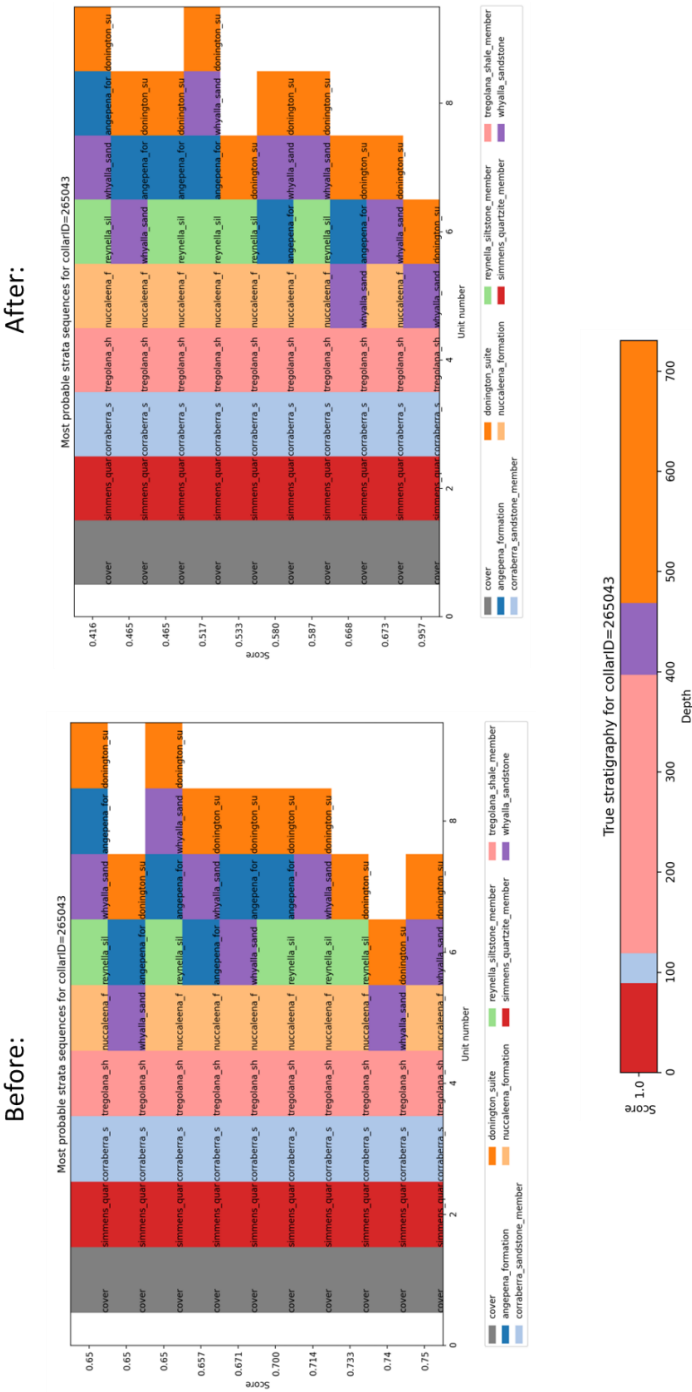
284



285 Finally, we can then include the depths to contacts between units in the drillhole based on the  
286 previous analyses (Fig. 9).



287  
288 Figure 9: The 12 most probable stratigraphic orderings showing true depth of contact (above)  
289 compared to the stratigraphy as logged for the same hole.  
290







294

295 In the next stage of our analysis, we perform solution correlation across multiple drill holes to  
296 establish a plausible stratigraphic order and reduce uncertainty. Figure 10 illustrates the comparison  
297 of the most probable stratigraphies before and after correlation. Prior to correlation, the solution  
298 that aligns with the “true” stratigraphy (the correct solution) is ranked second, with a score of  
299  $S=0.74$ , while the highest-ranked solution has a score of  $S=0.75$ . However, after applying the  
300 correlation, the correct solution rises to the top rank with a score of  $S=0.95$ , whereas the previously  
301 highest-ranked solution falls to second place with a score of  $S=0.67$ . This correlation analysis not only  
302 helped identify the correct solution but also significantly reduced its relative uncertainty, increasing  
303 the relative score between the top two solutions from 1% to 42%.

304

#### 305 4. Discussion and Future Work

306

307 Whilst we were able to develop a workflow that successfully provided useful stratigraphic analyses  
308 for our test area, we recognise that for other areas the methodology was not always as successful.  
309 We have identified several aspects of the current stratigraphic descriptions that we think will  
310 significantly expand the useability of the workflow we present above.

311 1) Lithological Uncertainty. The principal reason for this was that the lithological descriptions of  
312 stratigraphies in many areas is quite vague. Successive stratigraphic units in a group might  
313 have very similar lithological descriptions.

314 As an example, we look at the Hamersley Group, in Western Australia (Maldonado & Mercer,  
315 2018). If we examine the GSWA explanatory notes for three successive formations (Mt McRae  
316 Shale, Mt Sylvia Formation and the Wittenoom Formation) in the GSWA explanatory notes  
317 their lithologies are described as:

318 **Mt McRae Shale** - Mudstone, siltstone, chert, iron-formation, and dolomite. Thin  
319 bands of shard-bearing volcanic ash in upper parts.

320 **Mt Sylvia Formation** - Mudstone, siltstone, chert, iron-formation, and dolomite.

321 **Wittenoom Formation** - Thinly bedded dolomite and dolomitic shale, with minor  
322 black chert, shale, banded iron formation and sandstone.

323

324 We can see that there is a significant overlap in lithologies, with an ordering of lithologies but  
325 without constraints on the percentage of each lithology in the three formations. This  
326 additional information, even as an estimate, would provide useful constraints on the likelihood  
327 that a specific lithology is associated with a given stratigraphic unit.

328

329 2) Min-Max thickness estimates. In some areas, there is useful information on the minimum,  
330 maximum and average stratigraphic thickness of units.

331

332 3) Stratigraphic ordering of lithologies. Additional information on commonly occurring orderings  
333 of lithologies within a given formation or member would also provide useful constraints.



334

## West Angela Member

### Derivation of name/Formal lithostratigraphy

The West Angela Member was the first subdivision of the Wittenoom Formation to be formally recognized (Blockley et al., 1993). It is named after West Angela Hill (Zone 50, MGA 673387E 7442407N) near the West Angelas iron ore mine, and the type section is defined as the interval between 420.4 m and 524.6 m in drill hole WRL 1 (Blockley et al., 1993) stored at the Geological Survey of Western Australia (GSWA) Carlisle Core Library.

Five shaly horizons separated by BIF, chert, or massive dolomite are recognized in the West Angela Member and are informally designated as AS1 to AS5 (Kepert, 2018). In particular the lower three shale horizons form a distinctive pattern in natural gamma-ray logs that can be used for regional correlation (Blockley et al., 1993).

Minimum thickness (m) —  
Maximum thickness (m) 80

### Lithology

The West Angela Member is generally not well-exposed and consists predominantly of dolomite and shaly dolomite, with minor chert, BIF, volcanoclastic rocks, and impact ejecta layers. Near the base, there is a distinctive unit of interbedded chert, BIF, dolomitic shale, and shale with characteristic natural gamma-ray peaks that are designated AS1 to AS3 (Blockley et al., 1993). This entire interval is referred to as A1 by some mining companies (e.g. Kepert, 2018) and is overlain by a thick interval of shale and dolomitic shale (AS3). The middle of the member, between AS3 and AS 4, contains a unit of massive to laminated crystalline dolomite with local carbonaceous shale and siltstone partings (Blockley et al., 1993). The upper part of the West Angela Member (AS4 to AS5) consists mainly of dolomitic shale and shale with minor chert beds that is gradationally overlain by massive dolomite at the base of the Paraburdoo Member. Lateral correlations between drillholes WRL 1 and FVG 1 suggest that the member becomes shalier towards the east (Blockley et al., 1993).

335

336

Figure 11: Free-text descriptions of the West Angela Member in the GSWA Explanatory Notes.

337

All three of these types of information are often included in the free-text portions of stratigraphic databases, such as the example shown for the West Angela Member in the GSWA Explanatory Notes in Fig. 11. In this example the free-text provides more specific information on the thickness, the ordering of lithologies and the relative proportions of lithologies. With the advent of more sophisticated Machine Learning methodologies, the extraction of this ancillary data in a standardised form from reports and the stratigraphic databases themselves will open up new possibilities for constraining stratigraphy. Similarly, the codes developed in dh2loop for harmonising lithological terminologies will expand greatly in coming years.

340

341

342

343

344

345

4) Inclusion of discontinuity information in the litho2strat workflow (most often logged faults) could help to define where breaks in stratigraphy are most likely to occur

346

347

348

5) Inclusion of secondary descriptive information (for example grain size) could help to refine our younging estimators in areas of uncertain facing.

349

350

351

6) There is no doubt that the advent of Large Language Models will have a profound effect on our ability to extract and categorize information from unstructured data sources, and algorithms based on these approaches will probably replace the data extraction and data harmonisation modules in future versions of this workflow.

352

353

354

355

356

357



## 358 5. Conclusions

359

360 We developed codes and methodologies for stratigraphy recovery from drillhole databases, utilizing  
361 the branch and bound algorithm as a foundational framework. To ensure the generation of  
362 geologically plausible solutions, we implemented various types of constraints that account for the  
363 complexities of subsurface geology.

364 To further reduce uncertainty in the obtained solutions, we introduced a correlation algorithm that  
365 leverages information from multiple drillholes simultaneously. This innovative approach allows for a  
366 more robust analysis by integrating data across different locations, enhancing the reliability of the  
367 stratigraphic interpretations.

368 Our proposed method was applied to a dataset comprising 52 drillholes from South Australia. The  
369 results demonstrated that the algorithm successfully predicts the correct stratigraphic solution while  
370 providing associated uncertainty metrics, effectively validating its performance against measured  
371 stratigraphy data.

372 Additionally, we identified several key aspects of the current stratigraphic descriptions that could  
373 significantly enhance the usability of the workflow we have presented. These enhancements aim to  
374 improve the accessibility and applicability of our methodology, paving the way for more effective  
375 geological assessments and decision-making processes in the field.

376

377

378

379

380

381

382

383

384

385

386

387

388

389

390

391

392



393 *Code and data availability.* The software and datasets used in this study are publicly available for  
394 download at GitHub (<https://github.com/Loop3D/litho2strat>) and Zenodo  
395 (<https://doi.org/10.5281/zenodo.15064469>, Ogarko et al., 2025).

396 *Author contribution.* VO and MJ are the primary contributors to this study. VO led the research,  
397 developed the methodology and software, and prepared the manuscript. MJ provided guidance on  
398 drillhole data analysis and contributed to manuscript writing.

399 *Competing interests.* The authors declare that they have no conflict of interest.

400 *Acknowledgements.* The work has been supported by the Mineral Exploration Cooperative Research  
401 Centre whose activities are funded by the Australian Government's Cooperative Research Centre  
402 Program. This is MinEx CRC Document 20\*\*/\*\*.



## 403 Appendix A- Control file for litho2strat code

404

405 Example usage: `python3 litho2strat.py -p ./parfiles/Parfile_SA.txt`

406

407 Example parfile:

```
[FilePaths]¶
topology_filename = data/SA_test_data/newpairs_20_06_2023.gml¶
cover_unit_filename = ¶
ignore_list_filename = data/SA_test_data/ignore_list.txt¶
alternative_rock_names_filename = data/SA_test_data/alternative_rock_names.txt¶
unit_colors_filename = data/SA_test_data/unit_colors.csv¶
¶
drillsample_filename = data/SA_test_data/litho_tables/litho_${collarID$.csv¶
stratasample_filename = data/SA_test_data/strat_tables/strat_${collarID$.csv¶
dist_table_filename = data/SA_test_data/dh_asud_strat2.csv¶
¶
[DataHeaders]¶
drillsample_header = DEPTH_FROM_M, DEPTH_TO_M, MAJOR_LITHOLOGY, ¶
stratasample_header = DEPTH_FROM_M, DEPTH_TO_M, STRAT_UNIT_NAME, ¶
strata_data_header = strat, summary, distance, description¶
¶
[SolverParameters]¶
add_topology_constraints = True¶
max_num_strata_jumps = 0¶
max_num_returns_per_unit = 0¶
max_num_unit_contacts_inside_litho = 0¶
single_top_unit = True¶
¶
[Correlation]¶
correlation_power = 1.0¶
¶
[DataPreprocessing]¶
number_nearest_units = 10¶
min_drillhole_litho_score = 80¶
group_drillhole_lithos = False¶
cover_ratio_threshold = 0.65¶
¶
[CollarIDs]¶
collarIDs = 265003,265010,265018,265030,265043,265051¶
```

408

409

410

411

412

413

414

415



- 416 Alvarado-Neves, F., Ailleres, L., Grose, L., Cruden, A. R., & Armit, R. (2024). Three-dimensional  
417 geological modelling of igneous intrusions in LoopStructural v1.5.10. *Geoscientific Model*  
418 *Development*, 17(5), 1975–1993. <https://doi.org/10.5194/gmd-17-1975-2024>
- 419 Calcagno, P., Chilès, J. P., Courrioux, G., & Guillen, A. (2008). Geological modelling from field data and  
420 geological knowledge. *Physics of the Earth and Planetary Interiors*, 171(1–4), 147–157.  
421 <https://doi.org/10.1016/j.pepi.2008.06.013>
- 422 Caumon, G., Collon-Drouaillet, P., Le Carlier de Veslud, C., Viseur, S., & Sausse, J. (2009). Surface-  
423 Based 3D Modeling of Geological Structures. *Mathematical Geosciences*, 41(8), 927–945.  
424 <https://doi.org/10.1007/s11004-009-9244-2>
- 425 D’Afonseca, F. M., Finkel, M., & Cirpka, O. A. (2020). Combining implicit geological modeling, field  
426 surveys, and hydrogeological modeling to describe groundwater flow in a karst aquifer.  
427 *Hydrogeology Journal*, 28(8), 2779–2802. <https://doi.org/10.1007/s10040-020-02220-z>
- 428 Giraud, J., Pakyuz-Charrier, E., Jessell, M., Lindsay, M., Martin, R., & Ogarko, V. (2017). Uncertainty  
429 reduction through geologically conditioned petrophysical constraints in joint inversion.  
430 *GEOPHYSICS*, 82(6), ID19–ID34. <https://doi.org/10.1190/geo2016-0615.1>
- 431 Guo, J., Wang, Z., Li, C., Li, F., Jessell, M. W., Wu, L., & Wang, J. (2022). Multiple-Point Geostatistics-  
432 Based Three-Dimensional Automatic Geological Modeling and Uncertainty Analysis for  
433 Borehole Data. *Natural Resources Research*, 31(5), 2347–2367.  
434 <https://doi.org/10.1007/s11053-022-10071-6>
- 435 Guo, J., Xu, X., Wang, L., Wang, X., Wu, L., Jessell, M., Ogarko, V., Liu, Z., & Zheng, Y. (2024). GeoPDNN  
436 1.0: a semi-supervised deep learning neural network using pseudo-labels for three-dimensional  
437 shallow strata modelling and uncertainty analysis in urban areas from borehole data.  
438 *Geoscientific Model Development*, 17(3), 957–973. <https://doi.org/10.5194/gmd-17-957-2024>
- 439 Hagberg, A. A., Schult, D. A., & Swart, P. J. (2008). *Exploring Network Structure, Dynamics, and*  
440 *Function using NetworkX*. 11–15. <https://doi.org/10.25080/TCWV9851>
- 441 Hartmann, J., & Moosdorf, N. (2012). The new global lithological map database GLiM: A  
442 representation of rock properties at the Earth surface. *Geochemistry, Geophysics, Geosystems*,  
443 13(12). <https://doi.org/10.1029/2012GC004370>
- 444 Himsolt, M. (1997). *GML: a portable graph file format*.
- 445 Jessell, M. (2001). Three-dimensional geological modelling of potential-field data. *Computers &*  
446 *Geosciences*, 27(4), 455–465. [https://doi.org/10.1016/S0098-3004\(00\)00142-4](https://doi.org/10.1016/S0098-3004(00)00142-4)
- 447 Jessell, M., Aillères, L., Kemp, E. de, Lindsay, M., Wellmann, F., Hillier, M., Laurent, G., Carmichael, T.,  
448 & Martin, R. (2014). Next Generation Three-Dimensional Geologic Modeling and Inversion. In  
449 *Building Exploration Capability for the 21st Century*. Society of Economic Geologists.  
450 <https://doi.org/10.5382/SP.18.13>
- 451 Jessell, M., Ogarko, V., de Rose, Y., Lindsay, M., Joshi, R., Piechocka, A., Grose, L., de la Varga, M.,  
452 Ailleres, L., & Pirot, G. (2021). Automated geological map deconstruction for 3D model  
453 construction using `map2loop` and `map2model`. 1.0 and  
454 `map2model`. 1.0. *Geoscientific Model Development*,  
455 14(8), 5063–5092. <https://doi.org/10.5194/gmd-14-5063-2021>



- 456 Jessell, M. W., Ailleres, L., & de Kemp, E. A. (2010). Towards an integrated inversion of geoscientific  
457 data: What price of geology? *Tectonophysics*, 490(3–4), 294–306.  
458 <https://doi.org/10.1016/j.tecto.2010.05.020>
- 459 Joshi, R., Madaiah, K., Jessell, M., Lindsay, M., & Pirot, G. (2021).  
460 &lt;i>dh2loop</i>: an open-source Python library for  
461 automated processing and classification of geological logs. *Geoscientific Model Development*,  
462 14(11), 6711–6740. <https://doi.org/10.5194/gmd-14-6711-2021>
- 463 Land, A. H., & Doig, A. G. (1960). An Automatic Method of Solving Discrete Programming Problems.  
464 *Econometrica*, 28(3), 497. <https://doi.org/10.2307/1910129>
- 465 Lindsay, M. D., Jessell, M. W., Ailleres, L., Perrouty, S., de Kemp, E., & Betts, P. G. (2013). Geodiversity:  
466 Exploration of 3D geological model space. *Tectonophysics*, 594, 27–37.  
467 <https://doi.org/10.1016/j.tecto.2013.03.013>
- 468 Maldonado, A., & Mercer, K. (2018). *Comparison of the Laboratory and Barton-Bandis Derived Shear*  
469 *Strength of Bedding Partings in Fresh Shales of the Pilbara, Western Australia. All Days*, ISRM-  
470 ARMS10-2018-204.
- 471 Mallet, J.-L. L. (2002). *Geomodeling*. Oxford University Press, Inc.
- 472 Martin, R., Ogarko, V., Giraud, J., Plazolles, B., Angrand, P., Rousse, S., & Macouin, M. (2024). Gravity  
473 data inversion of the Pyrenees range using Taguchi sensitivity analysis and ADMM bound  
474 constraints based on seismic data. *Geophysical Journal International*, 240(1), 829–858.  
475 <https://doi.org/10.1093/gji/ggae410>
- 476 Ogarko, V., Giraud, J., Martin, R., & Jessell, M. (2021). Disjoint interval bound constraints using the  
477 alternating direction method of multipliers for geologically constrained inversion: Application to  
478 gravity data. *GEOPHYSICS*, 86(2), G1–G11. <https://doi.org/10.1190/geo2019-0633.1>
- 479 Ogarko, V., & Jessell, M. (2025). litho2strat 1.0 source code,  
480 <https://doi.org/10.5281/zenodo.15064469>
- 481 Pakyuz-Charrier, E., Giraud, J., Ogarko, V., Lindsay, M., & Jessell, M. (2018). Drillhole uncertainty  
482 propagation for three-dimensional geological modeling using Monte Carlo. *Tectonophysics*,  
483 747–748, 16–39. <https://doi.org/10.1016/j.tecto.2018.09.005>
- 484 Schetselaar, E. M., & Lemieux, D. (2012). A drill hole query algorithm for extracting lithostratigraphic  
485 contacts in support of 3D geologic modelling in crystalline basement. *Computers & Geosciences*,  
486 44, 146–155. <https://doi.org/10.1016/j.cageo.2011.10.015>
- 487 Tarantola, A. (2005). *Inverse Problem Theory and Methods for Model Parameter Estimation*. Society  
488 for Industrial and Applied Mathematics. <https://doi.org/10.1137/1.9780898717921>
- 489 Vollgger, S. A., Cruden, A. R., Ailleres, L., & Cowan, E. J. (2015). Regional dome evolution and its  
490 control on ore-grade distribution: Insights from 3D implicit modelling of the Navachab gold  
491 deposit, Namibia. *Ore Geology Reviews*, 69, 268–284.  
492 <https://doi.org/10.1016/j.oregeorev.2015.02.020>
- 493 Wellmann, F., & Caumon, G. (2018). *3-D Structural geological models: Concepts, methods, and*  
494 *uncertainties* (pp. 1–121). <https://doi.org/10.1016/bs.agph.2018.09.001>
- 495